Spent Coffee Ground-Based Materials Evaluated by Methylene Blue Removal

Andrea Mariela Araya-Sibaja [1,2] , Tamara Quesada-Soto [1], José Roberto Vega-Baudrit [1] ,
Mirtha Navarro-Hoyos [3,4] , Johnny Valverde-Cerdas [5] and Luis Guillermo Romero-Esquivel [5,*]

1 National Laboratory of Nanotechnology LANOTEC-CeNAT-CONARE, Pavas, San José 1174-1200, Costa Rica;
   aaraya@cenat.ac.cr (A.M.A.-S.); tamaraqs@hotmail.es (T.Q.-S.); jvegab@gmail.com (J.R.V.-B.)
2 Technical University of Costa Rica (UTN), Sede Central, Alajuela 159-7050, Costa Rica
3 Bioactivity for Sustainable Development (BIODESS), Department of Chemistry, University of Costa
   Rica (UCR), Rodrigo Facio Campus, San Pedro Montes Oca, San José 2060, Costa Rica; mnavarro@codeti.org
4 Chemistry Department, Georgetown University, Washington, DC 20057, USA
5 Environmental Protection Research Center (CIPA), School of Chemistry, Instituto Tecnológico de Costa
   Rica (ITCR), Cartago 159-7050, Costa Rica; jovalverde@itcr.ac.cr
* Correspondence: lromero@itcr.ac.cr; Tel.: +506-2550-2219

Abstract: Spent coffee grounds (SCG) are produced in large quantities during coffee brewing, contributing to environmental concerns. Additionally, cationic dyes from textile, paper, and leather wastewater pose a major pollution issue. This study explores SCG as an adsorbent for methylene blue (MB) dye. A novel comparison of SCG cleaning methods with warm water, accelerated solvent extraction (ASE), supercritical fluid extraction (SFE), and ultrasound-induced cavitation (US) is presented. In addition, the chemical modifications of SCG using acetylation, acid (HNO_3), and base (KOH) treatment that have not been reported before are presented. ATR-FTIR confirmed the inclusion of functional groups, for example, the nitro group in SCG treated with HNO_3, and an increase in carboxylic groups in the samples treated with KOH and HNO_3. SEM analysis revealed a consistent porous texture across samples, with SCG-SFE, SCG-US, and SCG-HNO_3 showing smaller pores, and SCG-ASE displaying elongated cavities. Adsorption isotherm tests followed the Freundlich and Langmuir models, indicating favorable adsorption. The Langmuir maximum adsorption capacity (q_{max}) varied among cleaning methods from 65.69 mg/g (warm water) to 93.32 mg/g (SFE). In contrast, in base- and acid-treated SCG, a three- to four-fold increase in adsorption capacity was observed, with q_{max} values of 171.60 mg/g and 270.64 mg/g, respectively. These findings demonstrate that SCG washed with warm water and chemically treated achieves adsorption capacities comparable to other biosorbents reported in the literature. Therefore, SCG represents a promising, low-cost, and sustainable material for removing cationic dyes from wastewater, contributing to waste valorization and environmental protection.

Keywords: spent coffee grounds; methylene blue adsorption capacity; cationic dyes; wastewater; circular economy

1. Introduction

Coffee is one of the most consumed beverages worldwide, generating vast quantities of waste in the form of spent coffee grounds (SCG) [1]. The amount of SCG generated worldwide per year is approximately 6 million tons [2]. Traditionally discarded, these residues contribute to environmental pollution and resource wastage [3]. Growing environmental concerns and the need for sustainable waste management practices have prompted

significant interest in the valorization of agricultural and food waste byproducts. In this context, SCG has emerged as a promising candidate for various applications due to its abundance, low cost, and unique physicochemical properties [3]. Notably, SCG possesses inherent characteristics such as high porosity, large surface area, and rich functional groups, making it suitable for absorbing a wide range of pollutants, including heavy metals, dyes, and organic compounds [4]. Recent research highlights the potential of SCG as an effective and eco-friendly adsorbent material for the removal of contaminants from water and wastewater [3–6]. Moreover, Ahsan et al. [7] indicated that the major components of SCG include cellulose and lignin containing polar and non-polar functional groups like hydroxyl, carboxylic, aldehydes, ketones, and ether, making them appropriate as an adsorbent for pollutants [7]. Furthermore, SCG can be a good alternative to activated carbon traditionally produced from non-renewable sources such as coal, for which the production is costly and environmentally unsustainable [8], contradicting the principles of sustainability and environmental preservation. From our perspective, utilizing SCG as a low-cost and effective adsorbent is more attractive and can significantly contribute to circular economy practices by transforming waste into valuable resources and addressing crucial environmental challenges.

There are reports in the literature on using SCG [5,9], chemically treated SCG [6,7,10], and the application of SCG as a raw material for the preparation of activated carbon [11–14]. Although, the latter practice is not consistent with environmentally friendly approaches. In the studies reported using only SCG [5,9], the material is washed with distilled water. However, warm water, accelerated solvent extraction (ASE), supercritical fluid extraction (SFE), and ultrasound-induced cavitation (US) present promising cleaning procedures that could enhance SCG adsorption capacity. To the best of our knowledge, no studies have tackled this issue. Regarding SCG, chemical treatment, phosphoric acid treatment [6], magnetic modification [10], and sulfuric acid [7] treatment have been reported. According to our literature review, SCG acetylation, KOH and HNO_3 treatment of SCG have not been reported.

In this study, we evaluated SCG, cleaned by different procedures and chemically treated, as an adsorbent for methylene blue (MB) from aqueous solutions. MB is classified as a cationic dye. Such dyes include azo dyes, solvent dyes, carbocyclic dyes, and methane dyes [15]. These dyes are known for their toxic effects, including mutagenicity, carcinogenicity, and acute or chronic toxicity in both aquatic organisms and humans [16]. Specifically, MB represents an environmental problem, as it is toxic to aquatic life, hinders photosynthesis by blocking sunlight, and some of its degradation products may be carcinogenic [1,13]. Moreover, methylene blue (MB) is commonly used as a template or model compound to evaluate cationic dye adsorption capacity of various materials due to its well-known properties and straightforward detection methods [9]. MB is used for dyeing fabrics in clothing and textile industries and for dyeing paper and leather, consequently, a large quantity of MB containing wastewater is discharged into groundwater and surface water [17].

According to Oladoye et al. (2022), several technologies including chemical/electrocoagulation, oxidation, photocatalyzed degradation, biodegradation, biocatalytic degradation, and adsorption processes have been studied for cationic dyes and MB removal [17]. Recent developments in cationic dye removal include photocatalyzed degradation using nanocomposite (CuWO4@MIL-101 (Fe)) [18], adsorption on graphene metal–organic frameworks (ZIF-67@GO) [19], and the development of poly (vynilidene fluoride) membranes in non-toxic and sustainable solvents [20]. Among the different techniques, adsorption has attracted attention due to its flexibility and simplicity of design, initial cost, and operational simplicity [21].

This contribution aims to assess the potential of SCG subject to several cleaning and chemical treatments for removing cationic dyes, using MB as a template. These strategies range from simple cleaning with warm water to accelerated solvent extraction (ASE), supercritical fluid extraction (SFE), and ultrasound-induced cavitation (US). The chemical treatment included three different approaches: acetylation, acid (HNO_3), and base (KOH). This study presents the first systematic comparison of the effects of multiple cleaning methods on the adsorption performance of SCG. The chemically treated methods evaluated have not been reported for SCG in the literature previously. More details on the cleaning and chemical treatment selection are presented as an overview in the Results and Discussion Section. The properties of the materials after the different treatments were studied by Attenuated Total Reflectance-Fourier Transform Infrared Spectroscopy (ATR-FTIR) and Scanning Electron Microscopy (SEM) images. Finally, isotherm studies were performed to determine the effect of the different treatments applied to SCG in the MB adsorption capacity and compared with the literature.

2. Materials and Methods

2.1. Chemicals and SCG

Sulfuric acid ($\geq$98%), potassium hydroxide ($\geq$98%), acetic acid ($\geq$99%), sodium bicarbonate ($\geq$97.5%), and methylene blue ($\geq$95%) were purchased from Sigma Aldrich (St. Louis, MO, USA). Nitric acid (69.5%,) and 1-propanol ($\geq$99%) were obtained from J.T. Baker (Phillipsburg, NJ, USA). Potassium phosphate monobasic ($\geq$99%) and sodium phosphate dibasic anhydrous ($\geq$99%) were purchased from Fisher chemical (Edmonton, AB, Canada) and Fermont (Monterrey, NL, Mexico), respectively. Spent coffee grounds (SCG) (<50% moisture, particle diameter range: 0.5–0.7 mm) was obtained from local coffee shops and was cleaned and chemically treated as indicated in the following sections.

2.2. Cleaning Procedures

2.2.1. Water Extraction

Firstly, 25.0 g of wet SCG, as obtained after coffee drink preparation, was cleaned by two successive extractions of 200 mL of hot water (70 °C) each. The process was performed with a standard commercial drip coffee maker, Oster brand, equipped with a fabric filter. Each extraction lasted approximately 3 to 5 min, corresponding to the time required to brew 200 mL. The sample was identified as SCG-H_2O.

2.2.2. Accelerated Solvent Extraction (ASE)

ASE was carried out on a Dionex™ASE™300 accelerated solvent extractor (ASE) (Thermo Scientific™, Walthman, MA, USA). A total of 5 g of SCG previously dried at 105 °C for 24 h was inserted into a 34 mL cell and extracted using a method consisting of 3 cycles of 10 min static time each, at a temperature of 120 °C, using 1-propanol as solvent without using diatomite. These conditions were selected based on previous experience of the research group [22–24] and the conditions reported by Efthymiopoulos et al. [25]. The sample was identified as SCG-ASE.

2.2.3. Supercritical Fluid Extraction (SFE)

SFE was performed using an SFT-110XW supercritical CO_2 extractor (Supercritical Fluid Technologies, Inc., Newark, DE, USA), equipped with a 100 mL volume extractor vessel. A total of 20 g of SCG previously dried at 105 °C for 24 h was placed inside the extractor vessel. The porous stainless-steel mesh filters were placed at both ends of the extractor vessel. Supercritical CO_2 extraction was carried out at 40 °C, 3625 psi, 14 mL/min

flow for 2 h [26]. The material obtained was identified as SCG-SFE and stored in a desiccator for further analyses.

2.2.4. Ultrasound-Induced Cavitation Process (US)

A total of 3 g of SCG-H_2O was placed in a beaker containing 80.0 mL of distilled water. Sonication was performed using a 20 Hz sonicator Q700 from QSonica (Newtown, CT, USA), equipped with a 6 mm titanium probe. The solution was sonicated with an amplitude of 40 for 30 min, using an on: off cycle of 45 s: 15 s to prevent excessive heating. The temperature was maintained at 25 °C with a water bath surrounding the beaker containing the solution [27]. The resulting solid was identified as SCG-US.

2.3. Chemical Treatment

The SCG samples subject to the water extraction procedure (SCG-H_2O) were further treated chemically as explained in the next sections.

2.3.1. Acetylation

Acetylated material (SCG-Acet) was prepared according to the procedure by Taleb et al. for the modification of lignin derived from spent coffee grounds [28]. For this stage, we used 10 g of SCG-H_2O. The material was placed in a 500 mL flask and 34 mL of acetic anhydride and approximately 1 mL of 98% (18 M) sulfuric acid were added. Then, the flask was connected to a vertical reflux condenser equipped with a recirculation bath and pump. The system was heated slowly until it reached boiling and maintained with a magnetic stirrer for approximately 3 h. After this time, the sample was left idle for 12 h and the water generated as a byproduct of the reaction was subsequently removed by distillation. The obtained material was washed and excess acid neutralized with 50 mL of sodium bicarbonate 10% solution. Neutralization was verified with pH paper after stirring the solution.

2.3.2. Acid Treatment

For acid-treated material (SCG-HNO_3), 100 mL of nitric acid 6 M was added to 40 g of SCG-H_2O and placed in an ultrasound bath for 1 h [29]. The supernatant was neutralized using sodium hydroxide and washed with water.

2.3.3. Basic Treatment

To obtain basic-treated material (SCG-KOH), 100 mL of potassium hydroxide 6 M was added to 40 g of SCG-H_2O and placed in an ultrasound bath for 3 h [30]. The supernatant was neutralized using hydrochloric acid and washed with water.

2.4. SCG-Based Materials Characterization
2.4.1. Attenuated Total Reflectance-Fourier Transform Infrared Spectroscopy (ATR-FTIR)

ATR-FTIR spectra were collected using 32 scans at a resolution of 4 cm^{-1} from a Thermo Scientific Nicolet iS50 spectroscope (Waltham, MA, USA). The instrument was equipped with a diamond attenuated total reflectance (ATR) accessory. The samples were situated directly into the ATR device and measured in the range of 4000–600 cm^{-1}, collecting 32 scans at a resolution of 4 cm^{-1}.

2.4.2. Scanning Electron Microscopy (SEM)

The surface morphology of the samples was determined using a JSM-6390 LV microscope from JEOL (Tokyo, Japan) operated at an acceleration voltage of 20 kV. The samples were mounted on metal stubs using double-sided adhesive tape and vacuum-coated with gold (350 Å) using a Denton Vacuum Desk V coating system.

2.5. Methylene Blue Adsorption Test

Duplicate adsorption isotherm experiments were carried out by placing different adsorbent doses (1, 2, 4, and 8 gL^{-1}) in contact with 25 mL of MB 100 mg/L solution in 100 mL glass bottles. The MB solutions were prepared using KH_2PO_4 and NaH_2PO_4, both 0.067 M, in a 4:6 mixture, respectively, as indicated in standard K 1474-1991 from Japan [31]. Before solution addition, solids were boiled with 3 mL of water to remove air trapped in its porous structure and to prevent the material floating. Once the material was observed at the bottom of the solution, the excess water was removed, and 25 mL of MB 100 mg/L concentration solution was added. The materials containing the solutions were agitated at 100 rpm at 25 °C in a Thermo Scientific Solaris shaker for 24 h. These parameters were defined based on Franca et al. (2009) [9]. The remaining concentration of MB was determined utilizing a Thermo Scientific Genesys 150 spectrophotometer, at a wavelength of 665 nm. The amount of MB adsorbed q_e (mgg^{-1}) was estimated using Equation (1):

$$q_e = \frac{(C_o - C_e) * V}{m} \tag{1}$$

where C_o (mgL^{-1}) is the initial MB concentration, C_e (mgL^{-1}) is the pseudo equilibrium MB concentration, V (L) is the volume of the MB solution, and m (g) is the mass of the adsorbent dry base.

The average values of q_e and C_e of duplicate test were used to determine the parameters of the Langmuir and Freundlich isotherms models (Equations (2) and (3), respectively) [32]:

$$q_e = \frac{q_{max} K_L C_e}{1 + K_L C_e} \tag{2}$$

where q_e (mgg^{-1}) and C_e (mgL^{-1}) are the adsorption capacity and the concentration of MB in equilibrium, respectively. q_{max} and K_L are the maximum adsorption capacity (mgg^{-1}) and the Langmuir constant (Lmg^{-1}), respectively.

Freundlich's model is given by Equation (3):

$$q_e = K_F C_e{}^n \tag{3}$$

where q_e (mgg^{-1}) and C_e (mgL^{-1}) are the adsorption capacity and the concentration of MB in equilibrium, respectively. K_F (mgg^{-1})(Lmg^{-1})^n is the adsorption coefficient and n is the dimensionless exponent.

The best fit model was selected by applying a non-linear chi-square (χ^2) together with the commonly used R^2 in Equations (4) and (5), respectively [33]:

$$\chi^2 = \sum \frac{(q_{e,exp} - q_{e,cal})^2}{q_{e,cal}} \tag{4}$$

$$R^2 = \frac{\sum (q_{e,mean} - q_{e,cal})^2}{\sum (q_{e,cal} - q_{e,mean})^2 + \sum (q_{e,cal} - q_{e,exp})^2} \tag{5}$$

where $q_{e,exp}$ (mgg^{-1}) is the amount of MB uptake at equilibrium obtained from Equation (1), $q_{e,cal}$ (mgg^{-1}) is the amount of adsorbate uptake achieved from the model, and $q_{e,mean}$ (mgg^{-1}) is the mean of the $q_{e,exp}$ values.

The calculation of Equations (2)–(5) was performed using the user interface (UI) for solving the non-linear adsorption isotherms and calculation of statistical parameter on Excel software for Microsoft 365 MSO (Version 2504) provided by [33].

3. Results and Discussion

3.1. Cleaning and Chemical Treatment Selection Overview

Adsorption phenomenon and its mechanisms depends on, among other factors, the characteristics of the adsorbate and the media, operation conditions, and, remarkably, the physicochemical characteristics of the adsorbent material [34]. Among the latter characteristics, the most important are large surface area, porosity, surface reactivity or chemistry, particle size, thermal and chemical stability, and hydrophilicity or hydrophobicity [35]. These attributes are crucial in designing and selecting adsorbent materials for specific applications, such as water purification, air filtration, and industrial waste treatment [34,35]. Therefore, to improve the SCG-based adsorbent's material properties, various cleaning and chemical treatment processes were evaluated.

In this context, since SCG is obtained after coffee drink preparation, substances such as caffeine, tannins, polyphenols, fatty acids, and others remained in the solid [36] which can interfere with the adsorption process [37]. Therefore, the first and most straightforward treatment to obtain an SCG-based material was the application of cleaning procedures. From the simplest extraction with hot water to advanced techniques such as ASE and SFE, these techniques were applied mainly for impurity removal, an increase in porosity, surface modification, improvements in selectivity, and chemical stability [38]. These could also be achieved by the unique properties of supercritical fluids as well as the high pressure and temperature applied to the solvents during ASE [39], which allow them to penetrate materials more effectively and rapidly than traditional solvents and solvent extractions [39,40]. This contributes to the removal and dissolution of impurities in a uniform way, modifying the surface and internal structure of the adsorbent [40]. Furthermore, the precise control over the extraction process in both techniques enabled the selective removal of specific compounds [41–43] that might interfere with adsorption [37]. Finally, these controlled conditions help in preserving the structural integrity and chemical stability of the adsorbent material, making it more durable and effective [39,40]. On the other hand, the US process, through its cavitation effect, enhances chemical reactions and ensures the efficient removal of contaminants. This process can increase adsorption sites and create or enlarge pores in SCG [44]. This technique has been successfully applied to improve the adsorption capacity of biochar derived from diverse biomass sources, effectively capturing and removing harmful substances [45].

Several chemical treatments have been extensively applied to improve the adsorption capacity of biosorbents [46]. For instance, the inclusion of several functional groups like carboxyl groups (COOH), carbonyl, and hydroxyl by nitric acid-treated rice husk residue has been reported [47]. In addition, depolymerization via nitration and oxidation was observed in lignin-based material treated with nitric acid [48]. Meanwhile, alkali treatment decomposes the covalent bonds between lignocellulose components by the depolymerization of hemicellulose and lignin [49], so that higher functional groups (hydroxyl and carboxyl groups) can be observed [50]. Furthermore, potassium hydroxide is widely used as an activating agent to create porous carbon-based materials due to its exceptional ability to produce a high specific surface area and significant pore volume [51]. Introducing acetyl groups has been shown to not only increase hydrophobicity and enhance surface area and porosity but also improve the binding efficiency of adsorbent materials [52]. This process enhances non-polar surface properties, thus improving the material's adsorption capacity for non-polar substances [53].

In sum, the selected treatments emphasize improving adsorption capacity by enlarging surface area, increasing porosity, enhancing surface reactivity or chemistry, and modifying hydrophilicity or hydrophobicity. This can be achieved by introducing or altering

functional groups on the material's surface, as well as improving adsorbate–adsorbent binding efficiency.

3.2. Attenuated Total Reflectance-Fourier Transformed Infrared Spectroscopy (ATR-FTIR)

Infrared spectroscopy is a powerful analytical technique widely used to identify functional groups and characterize chemical bonds in materials [54]. This method is particularly useful for assessing surface modifications, as it provides insights into molecular interactions and structural changes. In this study, infrared spectroscopy was employed to monitor the surface modification process of the SCG after cleaning and chemical treatment.

The ATR-FTIR signals identified in the SCG-H_2O material were similar to those previously reported in the literature for SCG of the Arabica coffee type [5,50,55,56] (Figure 1). The broad band at 3319 cm^{-1} related to O-H stretching of alcohols, phenols, and carboxylic acid groups [57,58] is characteristic of pectin, cellulose, hemicellulose, and lignin presence in this material [5,55]. Furthermore, SCG-H_2O showed a small and sharp peak at 3010 cm^{-1} related to =C–H stretch; two bands at 2921 and 2852 cm^{-1} associated with –C–H stretch; and bands at 1744 cm^{-1} and 1644 related to C=O stretching of the carbonyl groups of carboxylic acid, aldehydes, and esters functional groups [57,58]. Meanwhile, a broad band at 1529 cm^{-1} corresponded to the double bonds C=C of the aromatic structures [57,59]. In turn, signals at 1240 and 1156 cm^{-1} correspond to ester type –C–O stretching while 1030 cm^{-1} corresponds to alcohol type stretching [57,59]. Finally, bands at 864 and 815 cm^{-1} are distinctive of substitutions in aromatic structures present in lignin [57,59]. All these mentioned signals align with the presence of the main components of coffee waste: cellulose, hemicellulose, and lignin [5,54,55,60]. These signals were observed in the materials obtained through all cleaning procedures. However, SCG cleaned using ASE (SCG-ASE) exhibited an absence of the sharp peak at 3010 cm^{-1} related to =C–H stretching; a decreased intensity of peaks at 2921 and 2852 cm^{-1} related to aliphatic hydrocarbons stretching; and a disappearance of the band at 1744 cm^{-1} related to C=O stretching of the carbonyl groups in carboxylic acids, aldehydes, and esters. As reported by [25], such differences suggest that unsaturated fatty acids, ester linkages in lignin, and other carbonyl-containing compounds have been effectively removed by ASE [25]. Meanwhile, the signals associated with C=C stretching of aromatic double bonds at 1644 and 1529 cm^{-1} showed more intensity, in agreement with the more exposed lignin structure in the materials' surface. Unlike the cleaning process using ASE, the ATR-FTIR spectra of SCG-SFE and SCG-US showed intensification of the signals at 2921 and 2852 cm^{-1} and 1744 cm^{-1}, respectively, suggesting that both techniques were less efficient in removing fatty acids [26]. In this sense, Couto et al. (2009) have reported that the extraction of lipids from SCG using SFE is temperature and pressure dependent [26]. It is possible that the conditions used herein were unable to remove these compounds. Indeed, Couto and colleagues reported that the highest oil extraction yield was achieved at 50 °C and 4350 psi, which are higher temperature and pressure conditions than those used in this study (40 °C, 3625 psi). Additionally, the bands at 1644 cm^{-1}, associated with C=C stretching in lignin, along with the bands at 1380 and 1460 cm^{-1}, corresponding to C-H bending, and the band at 1030 cm^{-1}, related to C-O stretching in cellulose and hemicellulose, were also intensified in both SCG-SFE and SCG-US. This suggests that the SFE process, which employs CO_2, may selectively extract certain lipophilic compounds [42,43] while also inducing modifications in the functional groups present on the SCG surface. In line with these structural changes, the intensification of the signal at 3319 cm^{-1} observed in SCG-SFE and SCG-US further supports the occurrence of alterations in the hydrogen bonding network. This may be attributed to the removal of specific phenolic compounds from the SCG matrix by SFE, leading to the exposure of hydroxyl groups from polysaccharides such as cellulose and hemicellulose [41]. Interest-

ingly, ultrasonic cavitation may have induced comparable surface changes. The collapse of cavitation bubbles can facilitate the breakdown of hydrogen bonds and the rearrangement of the polymeric matrix [44], potentially exposing functional groups in a manner analogous to SFE. This parallel behavior indicates that, despite the different mechanisms of action, both SFE and US treatments led to similar structural modifications in the SCG matrix.
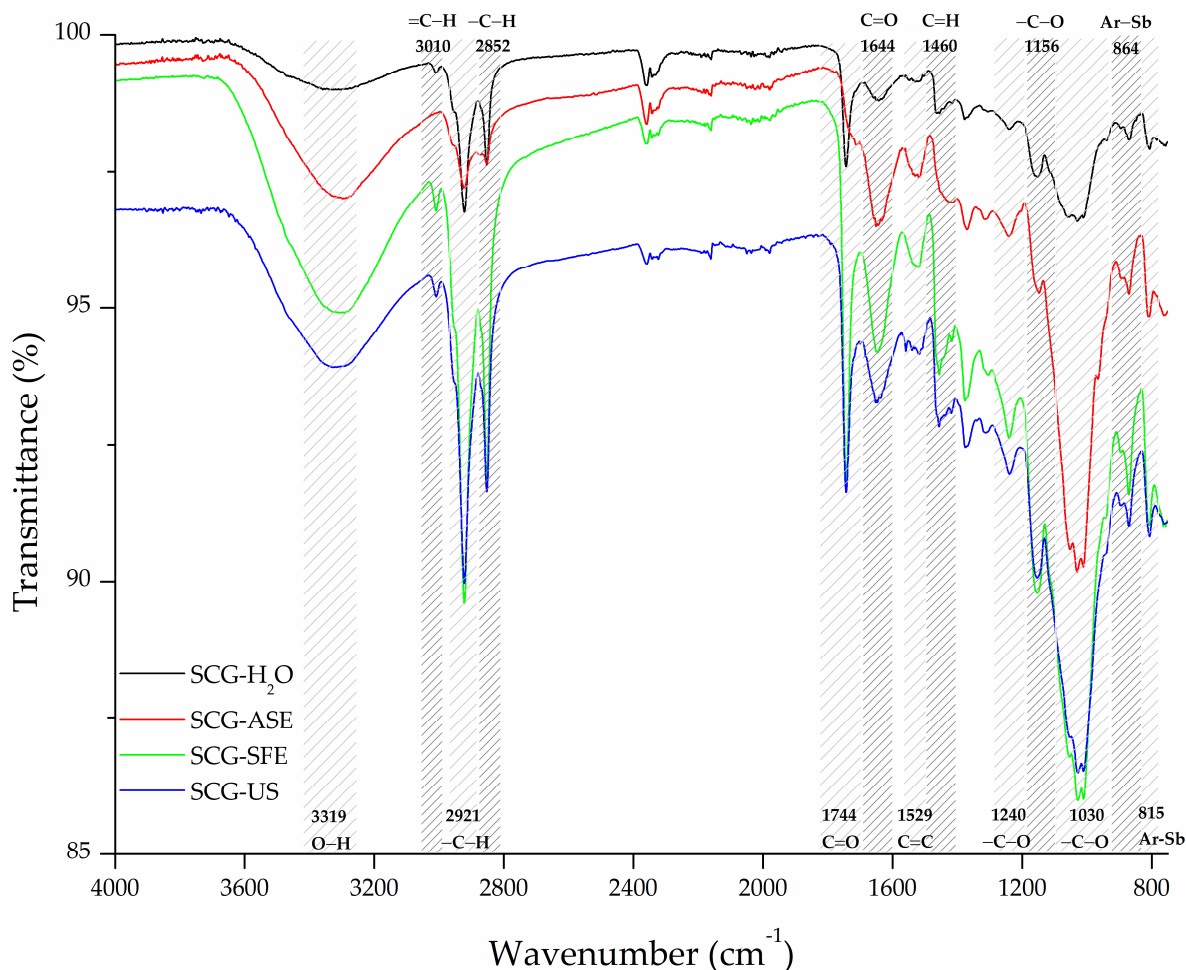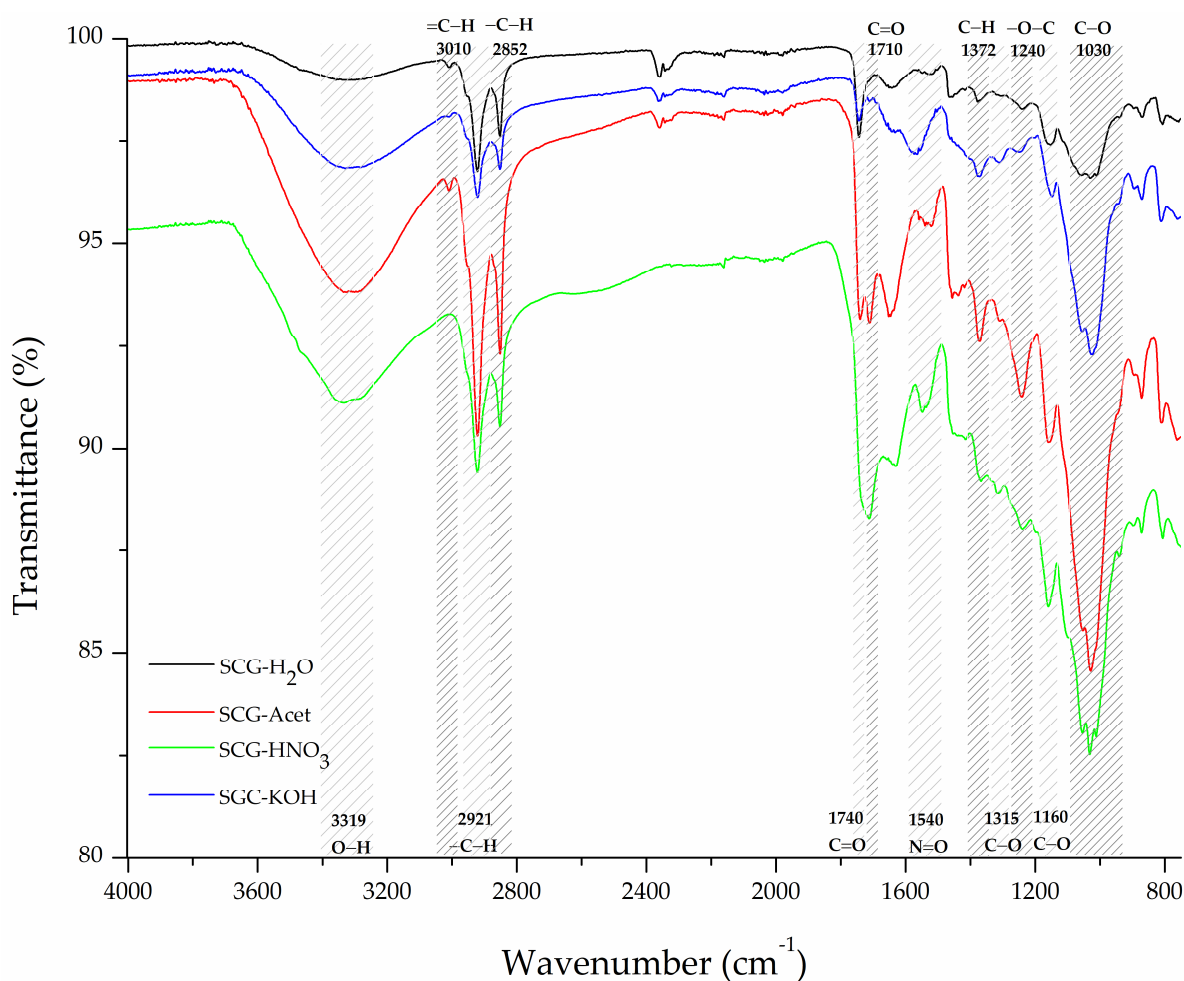

Figure 1. ATR-FTIR spectra of SCG-based materials after different cleaning procedures. (Ar-Sb refers to aromatic substitution).

Regarding chemical treatments, such as ATR-FTIR of the acetylated material, SCG-Acet in Figure 2 reveals the arising and increasing of new signals characteristic of the acetyl group. For example, an increase can be observed in the signals related to C-H bending at 1372 cm^{-1} in acetoxy moiety (-O(C=O)-CH$_3$) and—O-C stretching of the acetyl group (-C-O-CH$_3$) at 1240 cm^{-1} indicating the formation of ester linkages between the OH of SCG and acetic anhydride [52,61]. The signals in these two regions are key for determining successful acetylation of the material [52,61]. Acid treatment, on the other hand, is expected to add functional groups [47], cause oxidation, and, in this case, nitric acid can produce nitration [48] in the SCG surface. ATR-FTIR of SCG-HNO$_3$ showed signals consistent with these reactions. First, the lack of the signal at 3010 cm^{-1}, associated with =C–H stretching, indicated the breakdown of alkenes. Peaks associated with carbonyl groups around 1710 and 1740 cm^{-1} increased in intensity which is evidence of carboxylic acids formation. In addition, a new signal at 1540 cm^{-1} related to the N=O stretching vibrations of nitro compounds [57] suggests the nitration of the aromatic rings indicating the attachment of nitro groups (-NO$_2$) to the lignin structure. The oxidation of alcohols and the formation of new oxygen-containing groups were observed with the increment of intensity in signals at

1315, 1160, and 1030 cm^{-1} corresponding to C-O stretching in polysaccharides and other oxygenated groups [62]. In turn, alkali treatment (SCG-KOH) is estimated to provoke the breakdown of ester bonds, lignin degradation, deprotonation of acidic groups, and hydrolysis of organic matter. Ester bonds breakdown results in the formation of alcohols and carboxylate groups. Accordingly, an increase in the 3319 cm^{-1} band associated with O-H stretching of alcohol, the appearance of a band at 1572 cm^{-1} related to C=O stretching of carboxylate anions, and an increment in the signal at 1030 cm^{-1} associated with C-O stretching alcohol type [57] were observed, consistent with ester group saponification. The decrease in the small peak at 3010 cm^{-1} (=C–H stretching) and the signal around 2921 cm^{-1} corresponding to –C–H stretching in aliphatic chains can be attributed to the degradation of lignin, leading to lignin's aliphatic side chains or unsaturated linkages fragmenting [63].

Figure 2. ATR-FTIR spectra of SCG-based materials after different chemical treatments.

3.3. Scanning Electron Microscopy (SEM)

The surface morphology of all treated SCG samples was examined using SEM, with the resulting images presented in Figure 3. In addition to modifications in the chemical structure, the treatments performed could increase the surface area and porosity, thereby contributing to the adsorption capacity [6,44,50]. Almost all samples exhibited a consistent porous texture, characterized by the presence of holes and cavities, along with variations in surface smoothness and edge sharpness. Regarding the porous texture, SCG-SFE (Figure 3c), SCG-US (Figure 3d), and SCG-HNO$_3$ (Figure 3f), exhibited more holes and smaller pores compared with SCG-H$_2$O (Figure 3a).
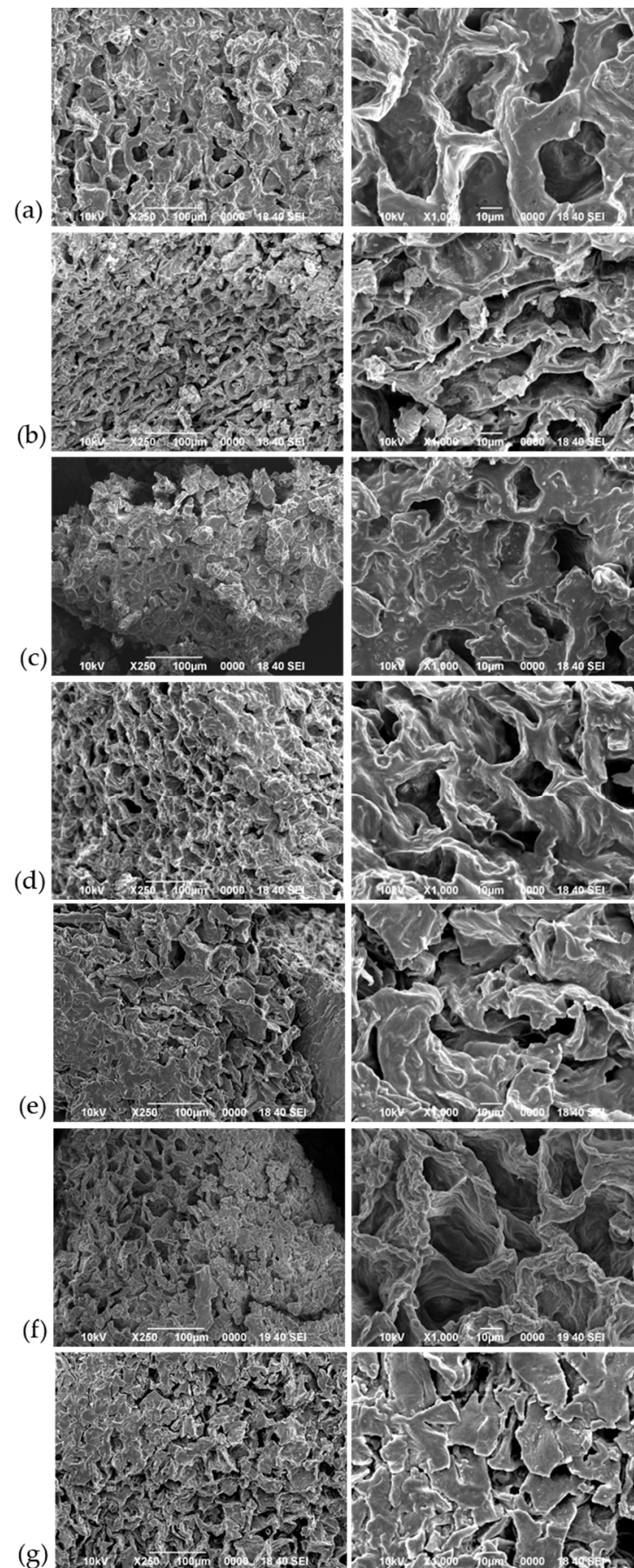
Figure 3. SEM images of SCG-based materials: (**a**) SCG-H_2O, (**b**) SCG-ASE, (**c**) SCG-SFE, (**d**) SCG-US, (**e**) SCG-Acet, (**f**) SCG-HNO_3, (**g**) SCG-KOH.

Notably, SCG-ASE (Figure 3b) exhibited elongated cavities, distinct from those observed in most of the other samples. This could be attributed to the selective interaction of 1-propanol with the material, where its directional flow under high pressure may have followed specific pathways, acting more aggressively in certain areas such as fiber bundles or lower density regions, ultimately resulting in pore elongation [64].

The acetylated sample (SCG-Acet, Figure 3e), and the sample modified with KOH (SCG-KOH, Figure 3g) showed a mixture of both angular and round shapes. These findings align with the effects of the treatments, which may have modified the surface morphology by closing the pores or forming a protective layer, while also removing soluble components and reducing pores size. Additionally, the treatments may have altered the cellulose structure, leading to decreased pores formation [65].

3.4. Adsorption Isotherms

The Langmuir and Freundlich data isotherm, including the statistical parameters, is shown in Table 1. Commonly, the best fitting isotherm model is determined with the coefficients of determination R^2. However, more statical parameters should be evaluated [33]. Tran et al. recommend calculating the chi-square (χ^2) together with the commonly used R^2 (Equations (4) and (5)) [66]. Accordingly, (χ^2) being close to zero indicates that the experimental and modeled data are similar. On the contrary, a high (χ^2) represents high bias between the experiment and the model. For all materials' isotherm data (Table 1), the Langmuir model R^2 (0.864–0.999) and χ^2 (0.35–13.21) were slightly higher and lower, respectively, than those of the Freundlich model (0.814–0.976 and 1.64–14.52, respectively). Thus, the Langmuir model vaguely better describes the MB adsorption in all the SCG samples tested. However, considering that the Freundlich and Langmuir statistical parameters are relatively close it is suggested that the binding sites on the adsorbent surface are both homogeneous and heterogenous [67], thus, both models are applicable.

Table 1. The Langmuir and Freundlich parameters for MB adsorption by the SCG materials studied.

Modification	Adsorbent	Langmuir				Freundlich			
		K_L (L/mg)	q_{max} (mg/g)	R^2	χ^2	K_F (mg/g)/ (L/mg)^n	n	R^2	χ^2
Cleaning	SCG-H$_2$O	0.051	65.69	0.993	0.35	7.03	0.48	0.958	1.64
	SCG-US	0.045	84.43	0.999	0.38	7.87	0.51	0.945	2.24
	SCG-ASE	0.041	83.19	0.995	0.33	8.23	0.48	0.949	2.46
	SCG-SFE	0.027	93.32	0.895	4.21	7.96	0.47	0.831	5.23
Chemical treatment	SCG-Acet	0.062	84.13	0.992	0.51	9.06	0.50	0.976	1.74
	SCG-KOH	0.015	171.60	0.978	1.96	4.24	0.73	0.959	3.11
	SCG-HNO$_3$	0.011	270.64	0.864	13.21	4.16	0.75	0.814	14.52

Consequently, some important insights can be obtained from the Freundlich data (Table 1). The Freundlich adsorption coefficient, K_F, was between 4.16 and 9.06 (mg/g)(L/mg)$^{1/n}$. The higher this parameter is, the higher the adsorbent loading [32]. The dimensionless n coefficients, a measure of adsorption intensity, ranged from 0.47 to 0.75 indicating favorable adsorption ($n < 1$) in all the materials [32]. Moreover, n below one indicates a high heterogeneity of the SCG surface materials and the existence of numerous binding sites with changing strengths on the adsorbent surface [68]. In general, both parameters, K_F and n indicate a good ability of the materials tested to remove MB from aqueous solutions.

The Langmuir model is related to equilibrium conditions of homogeneous monolayer adsorption [33,69]. Figure 4 presents the experimental data fitted to the Langmuir model

(best fitting one) of all the materials cleaned by different methods. Accordingly, they present similar actual experimental capacities in all the aqueous equilibrium MB concentration ranges. That is corroborated by the Langmuir model q_{max} values, within the same magnitude, between 65.69 and 93.32 mg/g (Table 1). However, the q_{max} of the SCG-H$_2$O is relatively lower than that obtained with other cleaning procedures; the application of such procedures could be limited due to higher energy, solvent consumption, or specialized equipment requirements. Therefore, the use of ASE, SFE, or US techniques is not justified given the minimal difference compared with water-extracted material.
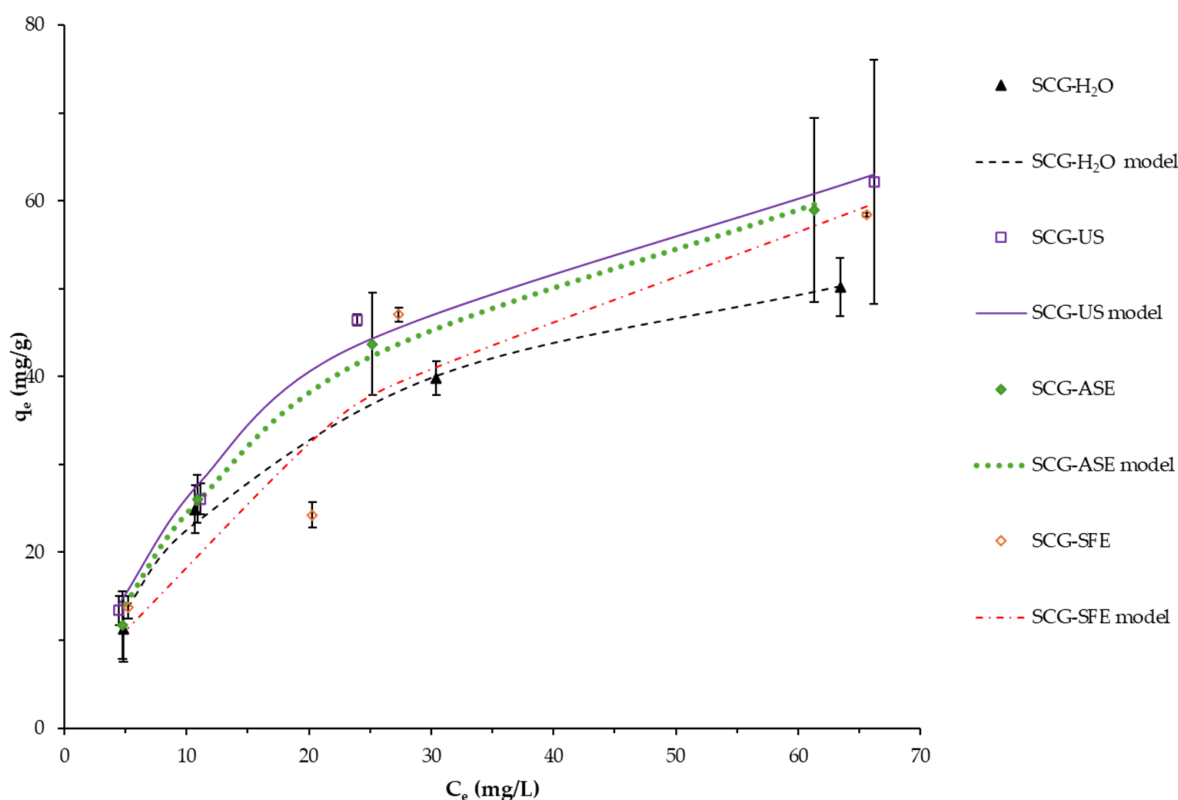
Figure 4. Adsorption isotherm and the Langmuir fitting model of MB by SCG cleaned by several procedures. Co: 100 mg/L, pH 7.0, T 25 °C, 130 rpm, 24 h contact time. Mean values and standard deviation error bars of duplicate tests are presented.

The chemically modified SCG is compared with the SCG-H$_2$O in Figure 5 and Table 1. Acetylation treatment produced materials with similar adsorption capacity to SCG-H$_2$O. The treatment with base and acid (KOH and HNO$_3$, respectively) was more effective and the adsorption capacity was increased around three- and four-fold, respectively. SCG-HNO$_3$ data must be used with caution, as the Langmuir and Freundlich data present lower R^2 and χ^2 values, indicating that the modification in the material surface and the incorporation of new functional groups (e.g., nitro) likely impact the isotherm model fit. Overall, according to the experimental and the modeled data, both acid and based treatment look promising. However, it is necessary to consider the chemical cost and the environmental and human health risks of handling dangerous chemical products.
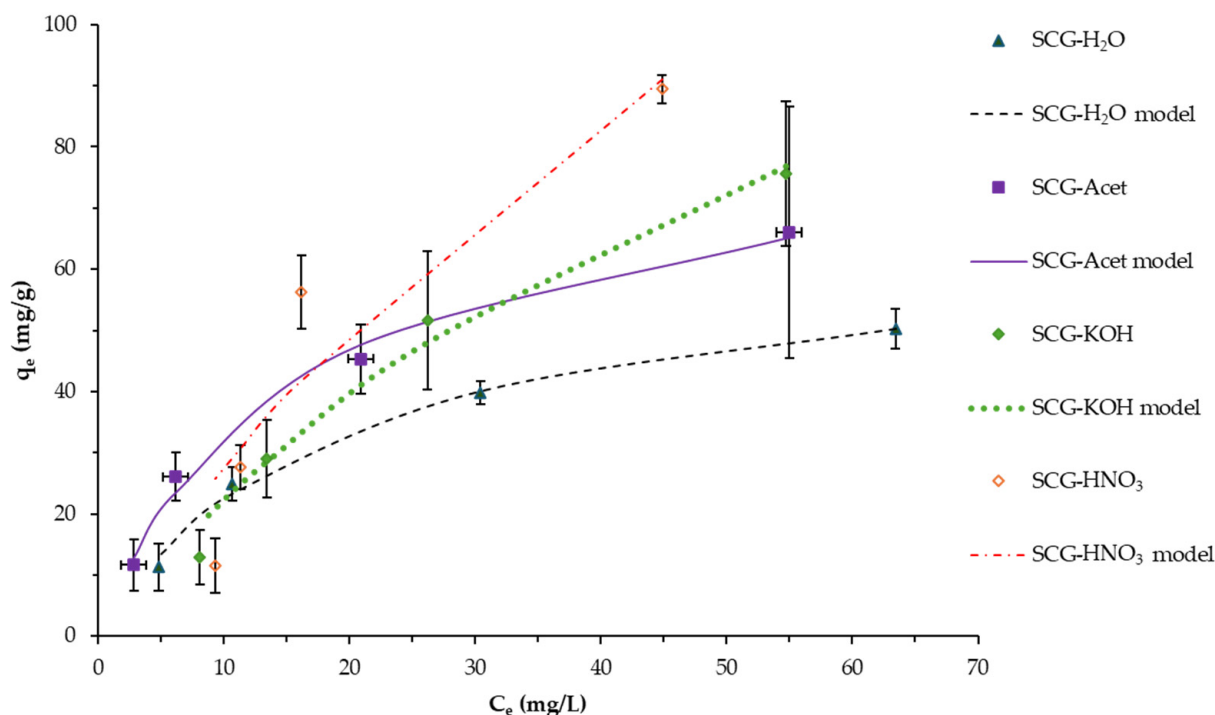
Figure 5. Adsorption isotherm and the Langmuir fitting model of MB by chemically treated SCG compared with SCG-H₂O. Co: 100 mg/L, pH 7.0, T 25 °C, 130 rpm, 24 h contact time. Mean values and standard deviation error bars of duplicate tests are presented.

The adsorption capacity observed in the different materials can be explained by the MB mechanism of adsorption influenced by the chemical composition of the adsorbent and chemical properties of MB. As shown by the ATR-FTIR spectra, the materials present hydroxyl, carbonyl, carboxyl, and aromatic moieties. Therefore, several interactions between MB and the different materials tested could be observed. Like other biosorbents, the predominant adsorption interactions include electrostatic and van der Waals interactions, hydrogen bonding, hydrophobic interaction, and π-π interactions [15]. As shown in the ATR-FTIR results (Figure 2), the HNO₃ and KOH treatment increased the formation of carboxylic groups (pKa 2.0–4.0) that can undergo dissociation and become negatively charged at pH above its pKa value. In this study, the adsorption experiment was performed at pH 7, while MB (pKa 3.8) was positively charged, favoring electrostatic interactions and, consequently, MB adsorption—as observed in the increased q_{max} values with respect to the non-treated SCG.

Table 2 shows the MB maximum adsorption capacity of various biomass adsorbents. The capacity of SCG-H₂O is close to the q_{max} reported by Dai et al. [70] and higher than other SCG studies (e.g., [9]). This can be explained by the differences in coffee species and roasting conditions, which result in different chemical compositions [2]. Moreover, the cleaning and testing procedures present some differences (e.g., pH and MB initial concentration). Compared with other biosorbents, SCG-H₂O capacity was higher than several other biosorbents listed in Table 2. Regarding the chemically treated materials, the q_{max} values of the SCG modified in this research were comparable, and in some cases superior, to the values reported in the literature (Table 3). In general, modified and non-modified SCG has the advantage of having a granular form, which is ideal for column filtration. On the contrary, most of the other materials are in powdered form, therefore, a granulation stage would be needed.

Table 2. Langmuir-based maximum adsorption capacity (Q_m) of several biosorbents.

Bioadsorbent	Contact Time (h)	Temperature (°C)	pH	C_o (mg/L)	Adsorbent Dose (g/L)	q_{max} (mg/g)	Reference
Sawdust from the European fan palm tree, *Chamaerops humilis*	2	25	8.0	20	N.A.	22.7	[71]
Waste orange peels	24	25	9.0	5–1000	6	40.13	[72]
Walnut shell	24	20	4.8	25–100	2.5	41.5	[73]
Peanut shell	24	20	4.8	25–100	2.5	46.8	[73]
Algerian Zean oak sawdust	0.75	25	7.0	20	1	52.376	[74]
Wild carob *Ceratonia siliqua*	24	20	N.A.	10–300	1	79.19	[75]
Waste pomegranate peels	24	25	9.0	5–1000	6	98.08	[72]
Waste banana peels	24	25	9.0	5–1000	4	112.35	[72]
Rubia tinctorum seeds	N.A.	25	5.0	N.A.	N.A.	125	[76]
Osage orange, *Maclura pomifera*	24	20	N.A.	10–300	1	146.92	[75]
Cowpea (*Vigna unguiculata* subsp. *unguiculata*) vines		30		N.A	0.5	149.25	[77]
Common bean (*Phaseolus vulgaris* L.) vine		30		N.A.	0.5	181.82	[77]
Grape pomace powder (GPP)	N.A.	20	N.A.	N.A	N.A.	183.96	[78]
Black cumin seeds	24	20	6.4	10–500	1	346.1	[79]
SCG	0.3	20	10	10–100	20	4.68	[80]
SCG	24	25	7.0	10–100	0.6	86.6	[70]
SCG	24	25	7.0	10–100	0.6	78.6	[70]
SCG	1	25	5.5	20–250	N.A.	40.85	[81]
SCG	12	25	5.0	50–500	10	18.7	[9]
SCG-H_2O	24	25	7.0	100	1, 2, 4, 8	64.56	This study

N.A.: not available.

Table 3. Langmuir-based maximum adsorption capacity (q_{max}) of several chemically modified biosorbents.

Modified Bioadsorbent	Contact Time (h)	Temperature (°C)	pH	C_o (mg/L)	Adsorbent Dose (g/L)	q_{max} (mg/g)	Reference
Abies marocana needles chemical treatment with sulfuric acid (H_2SO_4)	1	25	8.0	20–60	4	18.81	[82]
Modified peanut husk with $KMnO_4$	6	20	7.0	200	1	226	[83]
Magnetic sweet potato (*Ipomoea batatas* L.) peels	0.33	15	N.A.	100	20	38	[84]
Olive oil pomace, defatted with ethyl acetate	3.3	20	7.0	5–460	1	269	[85]
Sulfuric acid lignin (SAL) extracted from SCG	24	25	N.A.	10–100	1.2	66.225	[28]
Phenolated SAL extracted from SCG	24	25	N.A.	10–100	1.2	93.457	[28]
Acetylated SAL extracted from SCG	24	25	N.A.	10–100	1.2	71.942	[28]
Phosphorylated SCG (PSCG) (H_3PO_4/P_2O_5)	2	25	7.0	5–200	N.A.	188.68	[6]
Modified SCG with citric acid and polydopamine PDA@SC	24	25	7.0	60–100	0.33	291	[86]
SCG-Acet						60.14	
SCG-KOH	24	25	7.0	100	1, 2, 4, 8	165.47	This study
SCG-HNO$_3$						221.51	

4. Conclusions

In this study, the valorization of SCG as a carbonaceous adsorbent for MB was evaluated. Different cleaning procedures and chemical treatments for SCG not previously reported in the literature were applied to SCG. The former did not show any relevant changes in the morphology and chemical structure, supported by SEM images and ATR-FTIR spectra. However, an increase in carboxylic groups was observed in SCG treated with KOH and HNO_3. MB adsorption experiments showed favorable adsorption in all the materials (the Freundlich *n* coefficient was less than 1) and slightly best fitting of the Langmuir model to the data. The Langmuir maximum adsorption capacity of the SCG cleaned with water was comparable with other cleaning procedures like US, ASE, and SFE. Therefore, the water cleaning procedure is recommended, as less energy and no special equipment are needed. An increase in adsorption capacity was observed after treatment with KOH and HNO_3, likely related to the increase in carboxylic functional groups. Additionally, HNO_3 treatment generated more holes and smaller pores, as observed in SEM images, which may have contributed to its adsorption capacity. Overall, the non-treated and the chemically treated SCG samples presented MB adsorption capacities comparable with values reported in the literature for biosorbents. An economic, environmental, and human health risk assessment is recommended in the case of pursuing the chemical modification of SCG. In general, SCG presents in a granular form, making it ideal for wastewater column filtration without requiring additional granulation processes.

Author Contributions: Conceptualization, A.M.A.-S. and L.G.R.-E.; methodology, A.M.A.-S., T.Q.-S. and J.V.-C.; formal analysis, A.M.A.-S., T.Q.-S. and J.V.-C.; investigation, A.M.A.-S., J.V.-C. and L.G.R.-E.; resources, A.M.A.-S., L.G.R.-E., J.R.V.-B. and M.N.-H.; data curation, A.M.A.-S. and L.G.R.-E.; writing—original draft preparation, A.M.A.-S. and L.G.R.-E.; writing—review and editing, A.M.A.-S. and L.G.R.-E.; supervision, L.G.R.-E.; project administration, A.M.A.-S., L.G.R.-E. and M.N.-H.; funding acquisition, A.M.A.-S., L.G.R.-E., M.N.-H. and J.R.V.-B. All authors have read and agreed to the published version of the manuscript.

Data Availability Statement: The original contributions presented in this study are included in the article. Further inquiries can be directed to the corresponding author.

Conflicts of Interest: The authors declare no conflicts of interest.

References

1. Cuccarese, M.; Brutti, S.; De Bonis, A.; Teghil, R.; Di Capua, F.; Mancini, I.M.; Masi, S.; Caniani, D. Sustainable Adsorbent Material Prepared by Soft Alkaline Activation of Spent Coffee Grounds: Characterisation and Adsorption Mechanism of Methylene Blue from Aqueous Solutions. *Sustainability* **2023**, *15*, 2454. [CrossRef]
2. Franca, A.S.; Oliveira, L.S. Potential Uses of Spent Coffee Grounds in the Food Industry. *Foods* **2022**, *11*, 2064. [CrossRef] [PubMed]
3. Campos-Vega, R.; Loarca-Piña, G.; Vergara-Castañeda, H.A.; Oomah, B.D. Spent coffee grounds: A review on current research and future prospects. *Trends Food Sci. Technol.* **2015**, *45*, 24–36. [CrossRef]
4. Kovalcik, A.; Obruca, S.; Marova, I. Valorization of spent coffee grounds: A review. *Food Bioprod. Process.* **2018**, *110*, 104–119. [CrossRef]
5. Ballesteros, L.F.; Teixeira, J.A.; Mussatto, S.I. Chemical, Functional, and Structural Properties of Spent Coffee Grounds and Coffee Silverskin. *Food Bioproc. Technol.* **2014**, *7*, 3493–3503. [CrossRef]
6. Akindolie, M.S.; Choi, H.J. Surface modification of spent coffee grounds using phosphoric acid for enhancement of methylene blue adsorption from aqueous solution. *Water Sci. Technol.* **2022**, *85*, 1218–1234. [CrossRef]

7. Ahsan, M.A.; Jabbari, V.; Islam, M.T.; Kim, H.; Hernandez-Viezcas, J.A.; Lin, Y.; Díaz-Moreno, C.A.; Lopez, J.; Gardea-Torresdey, J.; Noveron, J.C. Green synthesis of a highly efficient biosorbent for organic, pharmaceutical, and heavy metal pollutants removal: Engineering surface chemistry of polymeric biomass of spent coffee waste. *J. Water Process Eng.* **2018**, *25*, 309–319. [CrossRef]

8. Rahimi, V.; Pimentel, C.H.; Gómez-Díaz, D.; Freire, M.S.; Lazzari, M.; González-Álvarez, J. Development and Characterization of Biomass-Derived Carbons for the Removal of Cu^{2+} and Pb^{2+} from Aqueous Solutions. *C* **2024**, *11*, 2. [CrossRef]

9. Franca, A.S.; Oliveira, L.S.; Ferreira, M.E. Kinetics and equilibrium studies of methylene blue adsorption by spent coffee grounds. *Desalination* **2009**, *249*, 267–272. [CrossRef]

10. Safarik, I.; Horska, K.; Svobodova, B.; Safarikova, M. Magnetically modified spent coffee grounds for dyes removal. *Eur. Food Res. Technol.* **2012**, *234*, 345–350. [CrossRef]

11. Campos, G.A.F.; Perez, J.P.H.; Block, I.; Sagu, S.T.; Celis, P.S.; Taubert, A.; Rawel, H.M. Preparation of Activated Carbons from Spent Coffee Grounds and Coffee Parchment and Assessment of Their Adsorbent Efficiency. *Processes* **2021**, *9*, 1396. [CrossRef]

12. Brazil, T.R.; Gonçalves, M.; Anjos, E.G.R.D.; de Oliveira Junior, M.S.; Rezende, M.C. Microwave-assisted production of activated carbon in an adapted domestic oven from lignocellulosic waste. *Biomass Convers. Biorefin.* **2024**, *14*, 255–268. [CrossRef]

13. Sukhbaatar, B.; Yoo, B.; Lim, J.-H. Metal-free high-adsorption-capacity adsorbent derived from spent coffee grounds for methylene blue. *RSC Adv.* **2021**, *11*, 5118–5127. [CrossRef]

14. Namane, A.; Mekarzia, A.; Benrachedi, K.; Belhanechebensemra, N.; Hellal, A. Determination of the adsorption capacity of activated carbon made from coffee grounds by chemical activation with ZnCl and HPO. *J. Hazard Mater.* **2005**, *119*, 189–194. [CrossRef] [PubMed]

15. Kanwal, A.; Rehman, R.; Imran, M.; Samin, G.; Jahangir, M.M.; Ali, S. Phytoremediative adsorption methodologies to decontaminate water from dyes and organic pollutants. *RSC Adv.* **2023**, *13*, 26455–26474. [CrossRef]

16. Lellis, B.; Fávaro-Polonio, C.Z.; Pamphile, J.A.; Polonio, J.C. Effects of textile dyes on health and the environment and bioremediation potential of living organisms. *Biotechnol. Res. Innov.* **2019**, *3*, 275–290. [CrossRef]

17. Oladoye, P.O.; Ajiboye, T.O.; Omotola, E.O.; Oyewola, O.J. Methylene blue dye: Toxicity and potential elimination technology from wastewater. *Results Eng.* **2022**, *16*, 100678. [CrossRef]

18. Khan, M.; Ahmed, M.M.; Akhtar, M.N.; Sajid, M.; Riaz, N.N.; Asif, M.; Kashif, M.; Shabbir, B.; Ahmad, K.; Saeed, M.; et al. Fabrication of CuWO4@MIL-101 (Fe) nanocomposite for efficient OER and photodegradation of methylene blue. *Heliyon* **2024**, *10*, e40546. [CrossRef]

19. Shah, H.U.R.; Ahmad, K.; Naseem, H.A.; Parveen, S.; Ashfaq, M.; Rauf, A.; Aziz, T. Water stable graphene oxide metal-organic frameworks composite (ZIF-67@GO) for efficient removal of malachite green from water. *Food Chem. Toxicol.* **2021**, *154*, 112312. [CrossRef]

20. Russo, F.; Marino, T.; Galiano, F.; Gzara, L.; Gordano, A.; Organji, H.; Figoli, A. Tamisolve® NxG as an Alternative Non-Toxic Solvent for the Preparation of Porous Poly (Vinylidene Fluoride) Membranes. *Polymers* **2021**, *13*, 2579. [CrossRef]

21. Yagub, M.T.; Sen, T.K.; Afroze, S.; Ang, H.M. Dye and its removal from aqueous solution by adsorption: A review. *Adv. Colloid Interface Sci.* **2014**, *209*, 172–184. [CrossRef] [PubMed]

22. Quirós-Fallas, M.I.; Vargas-Huertas, F.; Quesada-Mora, S.; Azofeifa-Cordero, G.; Wilhelm-Romero, K.; Vásquez-Castro, F.; Alvarado-Corella, D.; Sánchez-Kopper, A.; Navarro-Hoyos, M.; Characterization, P.H.R.S. Contents and Antioxidant Activity of Curcuma longa Rhizomes from Costa Rica. *Antioxidants* **2022**, *11*, 620. [CrossRef]

23. Vargas-Huertas, L.F.; Alvarado-Corella, L.D.; Sánchez-Kopper, A.; Araya-Sibaja, A.M.; Navarro-Hoyos, M. Characterization and Isolation of Piperamides from Piper nigrum Cultivated in Costa Rica. *Horticulturae* **2023**, *9*, 1323. [CrossRef]

24. Araya-Sibaja, A.M.; Vargas-Huertas, F.; Quesada, S.; Azofeifa, G.; Vega-Baudrit, J.R.; Navarro-Hoyos, M. Characterization, Antioxidant and Cytotoxic Evaluation of Demethoxycurcumin and Bisdemethoxycurcumin from Curcuma longa Cultivated in Costa Rica. *Separations* **2024**, *11*, 23. [CrossRef]

25. Efthymiopoulos, I.; Hellier, P.; Ladommatos, N.; Russo-Profili, A.; Eveleigh, A.; Aliev, A.; Kay, A.; Mills-Lamptey, B. Influence of solvent selection and extraction temperature on yield and composition of lipids extracted from spent coffee grounds. *Ind. Crops Prod.* **2018**, *119*, 49–56. [CrossRef]

26. Couto, R.M.; Fernandes, J.; da Silva, M.D.R.G.; Simões, P.C. Supercritical fluid extraction of lipids from spent coffee grounds. *J. Supercrit Fluids* **2009**, *51*, 159–166. [CrossRef]

27. Sompech, S.; Srion, A.; Nuntiya, A. The Effect of Ultrasonic Treatment on the Particle Size and Specific Surface Area of LaCoO3. *Procedia Eng.* **2012**, *32*, 1012–1018. [CrossRef]

28. Taleb, F.; Ammar, M.; Mosbah, M.B.; Salem, R.B.; Moussaoui, Y. Chemical modification of lignin derived from spent coffee grounds for methylene blue adsorption. *Sci. Rep.* **2020**, *10*, 11048. [CrossRef] [PubMed]

29. Chen, X.L.; Li, W.S.; Tan, C.L.; Li, W.; Wu, Y.Z. Improvement in electrochemical capacitance of carbon materials by nitric acid treatment. *J. Power Sources* **2008**, *184*, 668–674. [CrossRef]

30. Milanković, V.; Tasić, T.; Pašti, I.A.; Lazarević-Pašti, T. Resolving Coffee Waste and Water Pollution—A Study on KOH-Activated Coffee Grounds for Organophosphorus Xenobiotics Remediation. *J. Xenobiot.* **2024**, *14*, 1238–1255. [CrossRef]

31. *JIS K1474:2014*; Test Methods for Activated Carbon. Methylene Blue Adsorption Performance. JIS: Tokyo, Japan, 2014.

32. Worch, E. *Adsorption Technology in Water Treatment. Fundamentals, Processes, and Modeling*; Walter de Gruyter GmbH & Co.: Göttingen, Germany, 2012.

33. Wang, J.; Guo, X. Adsorption isotherm models: Classification; physical meaning, application and solving method. *Chemosphere* **2020**, *258*, 127279. [CrossRef] [PubMed]

34. Pellenz, L.; de Oliveira, C.R.S.; da Silva Júnior, A.H.; da Silva, L.J.S.; da Silva, L.; de Souza, A.A.U.; Ulson, S.M.D.A.G.; Borba, F.H.; da Silva, A. A comprehensive guide for characterization of adsorbent materials. *Sep. Purif. Technol.* **2023**, *305*, 122435. [CrossRef]

35. Pourhakkak, P.; Taghizadeh, M.; Taghizadeh, A.; Ghaedi, M. Adsorbent. In *Volume 33: Adsorption: Fundamental Processes and Applications*; Interface Science and Technology; Ghaedi, M., Ed.; Elsevier: Yasouj, Iran, 2021; pp. 71–210.

36. Mussatto, S.I.; Carneiro, L.M.; Silva, J.P.A.; Roberto, I.C.; Teixeira, J.A. A study on chemical constituents and sugars extraction from spent coffee grounds. *Carbohydr. Polym.* **2011**, *83*, 368–374. [CrossRef]

37. Satyam, S.; Patra, S. Innovations and challenges in adsorption-based wastewater remediation: A comprehensive review. *Heliyon* **2024**, *10*, e29573. [CrossRef]

38. Mane, P.V.; Rego, R.M.; Yap, P.L.; Losic, D.; Kurkuri, M.D. Unveiling cutting-edge advances in high surface area porous materials for the efficient removal of toxic metal ions from water. *Prog. Mater. Sci.* **2024**, *146*, 101314. [CrossRef]

39. Picot-Allain, C.; Mahomoodally, M.F.; Ak, G.; Zengin, G. Conventional versus green extraction techniques—A comparative perspective. *Curr. Opin. Food Sci.* **2021**, *40*, 144–156. [CrossRef]

40. Ibáñez, E.; Mendiola, J.A.; Castro-Puyana, M.; Extraction, S.F. *Encyclopedia of Food and Health*; Elsevier: Amsterdam, The Netherlands, 2016; pp. 227–233. [CrossRef]

41. Tyśkiewicz, K.; Konkol, M.; Rój, E. The Application of Supercritical Fluid Extraction in Phenolic Compounds Isolation from Natural Plant Materials. *Molecules* **2018**, *23*, 2625. [CrossRef]

42. Santoro, I.; Nardi, M.; Benincasa, C.; Costanzo, P.; Giordano, G.; Procopio, A.; Sindona, G. Sustainable and Selective Extraction of Lipids and Bioactive Compounds from Microalgae. *Molecules* **2019**, *24*, 4347. [CrossRef]

43. Vafaei, N.; Rempel, C.B.; Scanlon, M.G.; Jones, P.J.H.; Eskin, M.N.A. Application of Supercritical Fluid Extraction (SFE) of Tocopherols and Carotenoids (Hydrophobic Antioxidants) Compared to Non-SFE Methods. *AppliedChem* **2022**, *2*, 68–92. [CrossRef]

44. Belova, V.; Gorin, D.A.; Shchukin, D.G.; Möhwald, H. Controlled Effect of Ultrasonic Cavitation on Hydrophobic/Hydrophilic Surfaces. *ACS Appl. Mater. Interfaces* **2011**, *3*, 417–425. [CrossRef]

45. Wang, J.; Li, W.; Zhao, Z.; Musoke, F.S.N.; Wu, X. Ultrasonic Activated Biochar and Its Removal of Harmful Substances in Environment. *Microorganisms* **2022**, *10*, 1593. [CrossRef] [PubMed]

46. Martini, S.; Afroze, S.; Roni, K.A.; Setiawati, M.; Kharismadewi, D. A review of fruit waste-derived sorbents for dyes and metals removal from contaminated water and wastewater. *Desalination Water Treat* **2021**, *235*, 300–323. [CrossRef]

47. Hussain, M.; Ali, A.S.; Kousar, T.; Mahmood, F.; Haruna, A.; Zango, Z.U.; Adamu, H.; Kotp, M.G.; Abdulganiyyu, I.A.; Keshta, B.E. Efficient removal of manganese (II) ions from aqueous solution using biosorbent derived from rice husk. *Sustain. Chem. One World* **2025**, *5*, 100047. [CrossRef]

48. Karnitski, A.; Natarajan, L.; Lee, Y.J.; Kim, S.-S. Controlled chemical transformation of lignin by nitric acid treatment and carbonization. *Int. J. Biol. Macromol.* **2024**, *281*, 136408. [CrossRef]

49. Murthy, T.P.K.; Gowrishankar, B.S. Process optimisation of methylene blue sequestration onto physical and chemical treated coffee husk based adsorbent. *SN Appl. Sci.* **2020**, *2*, 836. [CrossRef]

50. Dávila-Guzmán, N.E.; de Jesús Cerino-Córdova, F.; Soto-Regalado, E.; Rangel-Mendez, J.R.; Díaz-Flores, P.E.; Garza-Gonzalez, M.T.; Loredo-Medrano, J.A. Copper Biosorption by Spent Coffee Ground: Equilibrium, Kinetics, and Mechanism. *Clean* **2013**, *41*, 557–564. [CrossRef]

51. El-Hendawy, A.-N.A. An insight into the KOH activation mechanism through the production of microporous activated carbon for the removal of Pb^{2+} cations. *Appl. Surf. Sci.* **2009**, *255*, 3723–3730. [CrossRef]

52. Onwuka, J.C.; Agbaji, E.B.; Ajibola, V.O.; Okibe, F.G. Thermodynamic pathway of lignocellulosic acetylation process. *BMC Chem.* **2019**, *13*, 79. [CrossRef]

53. Abegunde, S.M.; Idowu, K.S.; Adejuwon, O.M.; Adeyemi-Adejolu, T. A review on the influence of chemical modification on the performance of adsorbents, Resources. *Environ. Sustain.* **2020**, *1*, 100001. [CrossRef]

54. Xu, F.; Yu, J.; Tesso, T.; Dowell, F.; Wang, D. Qualitative and quantitative analysis of lignocellulosic biomass using infrared techniques: A mini-review. *Appl. Energy* **2013**, *104*, 801–809. [CrossRef]

55. Cerino-Córdova, F.J.; Dávila-Guzmán, N.E.; León, A.M.G.; Salazar-Rabago, J.J.; Soto-Regalado, E. Revalorization of Coffee Waste. In *Coffee-Production and Research*; IntechOpen: London, UK, 2020. [CrossRef]

56. Pujol, D.; Liu, C.; Gominho, J.; Olivella, M.À.; Fiol, N.; Villaescusa, I.; Pereira, H. The chemical composition of exhausted coffee waste. *Ind. Crops Prod.* **2013**, *50*, 423–429. [CrossRef]

57. Larkin, P. General Outline and Strategies for IR and Raman Spectral Interpretation. In *Infrared and Raman Spectroscopy*; Elsevier: Amsterdam, The Netherlands, 2011; pp. 117–133. [CrossRef]

58. Larkin, P. Environmental Dependence of Vibrational Spectra. In *Infrared and Raman Spectroscopy*; Elsevier: Amsterdam, The Netherlands, 2011; pp. 55–62. [CrossRef]

59. Larkin, P.J. IR and Raman Spectra–Structure Correlations. In *Infrared and Raman Spectroscopy*; Elsevier: Amsterdam, The Netherlands, 2018; pp. 85–134. [CrossRef]

60. Ottah, V.E.; Ezugwu, A.L.; Ezike, T.C.; Chilaka, F.C. Comparative analysis of alkaline-extracted hemicelluloses from Beech, African rose and Agba woods using FTIR and HPLC. *Heliyon* **2022**, *8*, e09714. [CrossRef] [PubMed]

61. El Boustani, M.; Brouillette, F.; Lebrun, G.; Belfkira, A. Solvent-free acetylation of lignocellulosic fibers at room temperature: Effect on fiber structure and surface properties. *J. Appl. Polym. Sci.* **2015**, *132*, 42247. [CrossRef]

62. Gieroba, B.; Kalisz, G.; Krysa, M.; Khalavka, M.; Przekora, A. Application of Vibrational Spectroscopic Techniques in the Study of the Natural Polysaccharides and Their Cross-Linking Process. *Int. J. Mol. Sci.* **2023**, *24*, 2630. [CrossRef]

63. de Carvalho Oliveira, F.; Srinivas, K.; Helms, G.L.; Isern, N.G.; Cort, J.R.; Gonçalves, A.R.; Ahring, B.K. Characterization of coffee (Coffea arabica) husk lignin and degradation products obtained after oxygen and alkali addition. *Bioresour. Technol.* **2018**, *257*, 172–180. [CrossRef]

64. Toda, T.A.; Santana, A.J.M.; Ferreira, J.A.; Pallone, E.M.D.J.A.; de Aguiar, C.L.; Rodrigues, C.E.D.C. Evaluation of Techniques for Intensifying the Process of the Alcoholic Extraction of Coffee Ground Oil Using Ultrasound and a Pressurized Solvent. *Foods* **2022**, *11*, 584. [CrossRef]

65. Aziz, T.; Farid, A.; Haq, F.; Kiran, M.; Ullah, A.; Zhang, K.; Li, C.; Ghazanfar, S.; Sun, H.; Ullah, R.; et al. A Review on the Modification of Cellulose and Its Applications. *Polymers* **2022**, *14*, 3206. [CrossRef]

66. Tran, H.N.; You, S.-J.; Hosseini-Bandegharaei, A.; Chao, H.-P. Mistakes and inconsistencies regarding adsorption of contaminants from aqueous solutions: A critical review. *Water Res.* **2017**, *120*, 88–116. [CrossRef]

67. Salifu, A.; Petrusevski, B.; Mwampashi, E.S.; Pazi, I.A.; Ghebremichael, K.; Buamah, R.; Aubry, C.; Amy, G.L.; Kenedy, M.D. Defluoridation of groundwater using aluminum-coated bauxite: Optimization of synthesis process conditions and equilibrium study. *J. Environ. Manag.* **2016**, *181*, 108–117. [CrossRef]

68. Farsad, A.; Niimi, K.; Ersan, M.S.; Gonzalez-Rodriguez, J.R.; Hristovski, K.D.; Westerhoff, P. Mechanistic Study of Arsenate Adsorption onto Different Amorphous Grades of Titanium (Hydr)Oxides Impregnated into a Point-of-Use Activated Carbon Block. *ACS EST Eng.* **2023**, *3*, 989–1000. [CrossRef]

69. Ali, K.; Zeidan, H.; Amar, R.B. Evaluation of the use of agricultural waste materials as low-cost and eco-friendly sorbents to remove dyes from water: A review. *Desalination Water Treat* **2023**, *302*, 231–252. [CrossRef]

70. Dai, Y.; Zhang, D.; Yan, H.; Ji, Y.; Wu, W.; Tanaka, S. Study on the mechanism of methylene blue adsorption of spent coffee grounds. *Fresenius Environ. Bull* **2016**, *25*, 3423–3429.

71. El Malti, W.; Koteich, S.; Hijazi, A. Utilizing *Chamaerops humilis* in removing methylene blue dye from water: An effective approach. *RSC Adv.* **2024**, *14*, 24196–24206. [CrossRef]

72. Tolkou, A.K.; Tsoutsa, E.K.; Kyzas, G.Z.; Katsoyiannis, I.A. Sustainable use of low-cost adsorbents prepared from waste fruit peels for the removal of selected reactive and basic dyes found in wastewaters. *Environ. Sci. Pollut. Res.* **2024**, *31*, 14662–14689. [CrossRef]

73. Lazarova, S.; Tonev, R.; Dimitrova, S.; Dimova, G.; Mihailova, I. Valorization of Peanut and Walnut Shells through Utilisation as Biosorbents for the Removal of Textile Dyes from Water. *Processes* **2023**, *11*, 2291. [CrossRef]

74. Sadoun, L.; Seffah, K.; Benmounah, A.; Zerizer, A.; Ghernaout, D. High-performance raw biosorbent derived from Algerian Zean oak sawdust for removing methylene blue from aqueous environments. *Desalination Water Treat* **2023**, *294*, 233–246. [CrossRef]

75. Bounaas, M.; Bouguettoucha, A.; Chebli, D.; Derbal, K.; Benalia, A.; Pizzi, A. Effect of Washing Temperature on Adsorption of Cationic Dyes by Raw Lignocellulosic Biomass. *Appl. Sci.* **2024**, *14*, 10365. [CrossRef]

76. Wardighi, Z.; Bensalah, J.; Zarrouk, A.; Rifi, E.H.; Lebkiri, A. Investigation of adsorption and mechanism of the cationic methylene blue by the polymeric Rubia tinctorum seeds from environment wastewater: Kinetic equilibrium and thermodynamic studies. *Desalination Water Treat* **2023**, *310*, 212–225. [CrossRef]

77. Qin, G.; Wang, C.; Yang, Q.; Wei, W. Removal of methylene blue from aqueous solution using common bean vine and cowpea vine biomass. *Desalination Water Treat* **2023**, *283*, 237–246. [CrossRef]

78. Colodel, C.; Canteli, A.M.D.; de Mello Castanho Amboni, R.D.; de Oliveira Petkowicz, C.L. Use of white grape pomace for removal of cationic dyes from aqueous solution: Kinetic, isotherm and thermodynamic characterization. *Biomass Convers. Biorefin.* **2024**. [CrossRef]

79. Benamraoui, F.; Boudiaf, H.; Bouhank, A.; Bencheikh, L.; Bourzami, R.; Gil, A.; Boulahbal, A.-I.; Boutahala, M. Methylene blue removal using black cumin seeds waste: Experimental study and molecular dynamic simulation. *Desalination Water Treat* **2023**, *300*, 167–177. [CrossRef]

80. Nitayaphat, W.; Jintakosol, T.; Engkaseth, K.; Wanrakakit, Y. Removal of methylene blue from aqueous solution by coffee residues. *Chiang Mai J. Sci.* **2015**, *42*, 407–416.

81. Nascimento, N.N.R.D.; da Trindade Silva, A.L.M.; Silva, W.L.; Rodrigues, M.G.F. Valorization of coffee agro-industrial residue for biochar production: Use as adsorbent for methylene blue removal. *Desalination Water Treat* **2024**, *320*, 100767. [CrossRef]

82. Zirari, M.; Aouji, M.; Hmouni, D.; El Mejdoub, N. Adsorption behavior and mechanism of modified *Abies marocana* Trab. needles for the efficient removal of methylene blue dye. *Water Pract. Technol.* **2024**, *19*, 3808–3832. [CrossRef]

83. Aryee, A.A.; Han, R.; Qu, L. Investigation into the adsorption of methylene blue and trimethoprim onto modified peanut husk in single and binary systems. *Desalination Water Treat* **2024**, *317*, 100248. [CrossRef]

84. Diagboya, P.N.; Odagwe, A.; Oyem, H.H.; Omoruyi, C.; Osabohien, E. Adsorptive decolorization of dyes in aqueous solution using magnetic sweet potato (*Ipomoea batatas* L.) peel waste. *RSC Sustain.* **2024**, *2*, 686–694. [CrossRef]

85. Hassani, E.M.S.; Duarte, H.; Brás, J.; Taleb, A.; Taleb, M.; Rais, Z.; Eivazi, A.; Norgren, M.; Romano, A.; Medronho, B. On the Valorization of Olive Oil Pomace: A Sustainable Approach for Methylene Blue Removal from Aqueous Media. *Polymers* **2024**, *16*, 3055. [CrossRef]

86. Tong, J.; Li, G.; Wei, J.; Li, C. Functionalized spent coffee grounds by citric acid and polydopamine for eliminating cationic dyes from wastewater: Investigation on recyclability, salt resistance and adsorption mechanism. *Ind. Crops Prod.* **2025**, *223*, 120198. [CrossRef]